Electroexcitation of ^{22}Ne below $E_x = 8.6$ MeV

X. K. Maruyama, F. J. Kline,* J. W. Lightbody, Jr., and S. Penner
Center for Radiation Research, National Bureau of Standards, Washington, D. C. 20234

W. J. Briscoe,† M. Lunnon,‡ and H. Crannell
The Catholic University of America, Washington, D. C. 20064

(Received 3 November 1978)

The states of ^{22}Ne below 8.6 MeV excitation energy have been studied using the technique of inelastic electron scattering. Ratios of inelastic to elastic scattering cross sections were measured with incident electron energies between 60 and 110 MeV and scattering angles of 110° and 128°. Form factors for 14 inelastic transitions were measured for the momentum transfer range 0.4 to 1.0 fm^{-1}. Reduced transition probabilities for these states have been deduced and assignments of spin and parity have been made.

[NUCLEAR REACTIONS ^{22}Ne(e,e'), $E=60$ to 110 MeV; measured $\sigma(E)$ at 110° and 128° up to 8.6 MeV in excitation energy; deduced J, π, $B(CL)$. Enriched ^{22}Ne target.]

I. INTRODUCTION

The spectroscopy of ^{22}Ne has been studied previously with hadronic probes. The α transfer reaction[1,2] ^{18}O(^{7}Li, t)^{22}Ne, the triton transfer reaction[2,3] ^{19}F($\alpha, p\gamma$)^{22}Ne, and the neutron stripping reaction[4] ^{21}Ne(d,p)^{22}Ne, among others, have made important contributions in recent years to determine the properties of the excited states of ^{22}Ne. A comparison of the assigned energies, spins, and parities of states in the 1973 and 1978 compilations[5,6] of Endt and Van der Leun shows many changes reflecting the growing understanding of the complex level structure of ^{22}Ne. Previous inelastic electron scattering experiments have been restricted to the study of the first excited state[7] and to magnetic transitions preferentially excited with 180° scattering.[8] The present experiment has employed a gas target cell design which allows an improved energy resolution and provides additional information concerning spin and parity of states in ^{22}Ne below particle emission threshold. In previous, lower resolution electron scattering experiments, the high level density in this excitation region was a severe limitation. The electromagnetic transition properties presented here should prove useful for those engaged in model calculations.

II. EXPERIMENTAL EQUIPMENT AND TECHNIQUE

The experiment was performed at the National Bureau of Standards electron linear accelerator. The data were taken at incident energies ranging from 60 to 110 MeV at nominal scattering angles of 110° and 128°. Typical overall experimental resolution was 0.13% full width at half maximum (FWHM) with currents up to several microamperes. The beam current was monitored with a Faraday cup. Scattered electrons were momentum analyzed in a 169.8° double focusing magnetic spectrometer and detected in a 48 detector hodoscope of Si(Li) solid state detectors. The spectrometer solid angle was nominally 4 msr. Details of the accelerator facility and detector system are found in Ref. 9.

The body of the target cell is a cylinder with inside diameter 1.27 cm and length 8.26 cm. The cylinder axis lies in the scattering plane, allowing transmission geometry to be used for the target orientation. The electron beam, with a typical area of 1×2 mm^2, was directed on the target. The detector system has transverse position sensitivity, so that electrons due to scattering from the gas and from the cell walls may be differentiated. A more complete description of the target cell characteristics is found in Ref. 10. The ^{22}Ne gas was isotopically enriched to greater than 90%. The pressure of the gas in the target ranged from 7 to 13 atmospheres absolute for the various runs corresponding to a ^{22}Ne target thickness between 8.2 and 15.2 mg/cm^2. In this experiment the ratio of inelastic to elastic cross sections was determined, obviating the need for a precise determination of the target dimensions.

III. DATA ANALYSIS

The inelastic cross sections were measured relative to the elastic cross section and then normalized to the calculated elastic cross sec-

TABLE I. Calculated phase shift elastic cross sections. Cross sections were calculated using a Fermi charge distribution (Ref. 12) with parameters $c = 2.782$ and $t = 2.412$.

E_0 (MeV)	θ (deg)	$\frac{\partial\sigma}{\partial\Omega}\left(\frac{\mu b}{sr}\right)$
59.59	110.39	51.33
69.69	110.45	27.66
69.91	110.39	27.47
85.13	110.36	10.67
100.34	110.36	3.907
110.61	110.28	1.888
63.84	128.16	13.39
77.42	128.17	5.296
110.56	128.05	0.398

tion for ^{22}Ne using the phase shift code HEINEL[11] with a two parameter Fermi distribution for the ground state charge distribution[12] with $c = 2.782$ fm and $t = 2.412$ fm. Table I presents the calculated elastic scattering cross sections. A spectrum of scattered electrons is shown in Fig. 1. In this example, the incident electron energy was 100 MeV and the scattering angle was 110°. The numbers shown above the observed peaks are the level identifications assigned in this work.

The peak areas were determined relative to the elastic peak by a nonlinear least squares fitting program which fits the elastic peak shape plus a polynomial background to the inelastic spectrum. Multiple inelastic peaks can be fitted simultaneously. The presence of the weaker peaks was determined by fitting the data with and without a peak in the region of the suspected peak. One-half of the change in χ^2 (because there are two parameters per peak) divided by the reduced χ^2 for the fit with the larger number of peaks is an F statistic.[13] The larger the value of F, the larger the probability that the observed change in χ^2 is due to a nonrandom fluctuation of the data, i.e., the greater the probability of the presence of an additional peak. For the data on the weaker states reported here, this probability was never smaller than 80% and in most cases greater than 99%. The assumption of identical peak shapes was deemed adequate, as the lowest particle emission threshold for α particles is at 9.67 MeV excitation energy and the resolution of the detection system does not change appreciably within this energy range. Table II tabulates the ratios of inelastic to elastic peak areas obtained in this experiment.

The inelastic electron scattering cross section

$$\left(\frac{d\sigma}{d\Omega}\right)_{\text{inel}} = \frac{\text{inelastic peak area}}{\text{elastic peak area}} \left(\frac{d\sigma}{d\Omega}\right)_{\text{el}} \qquad (3.1)$$

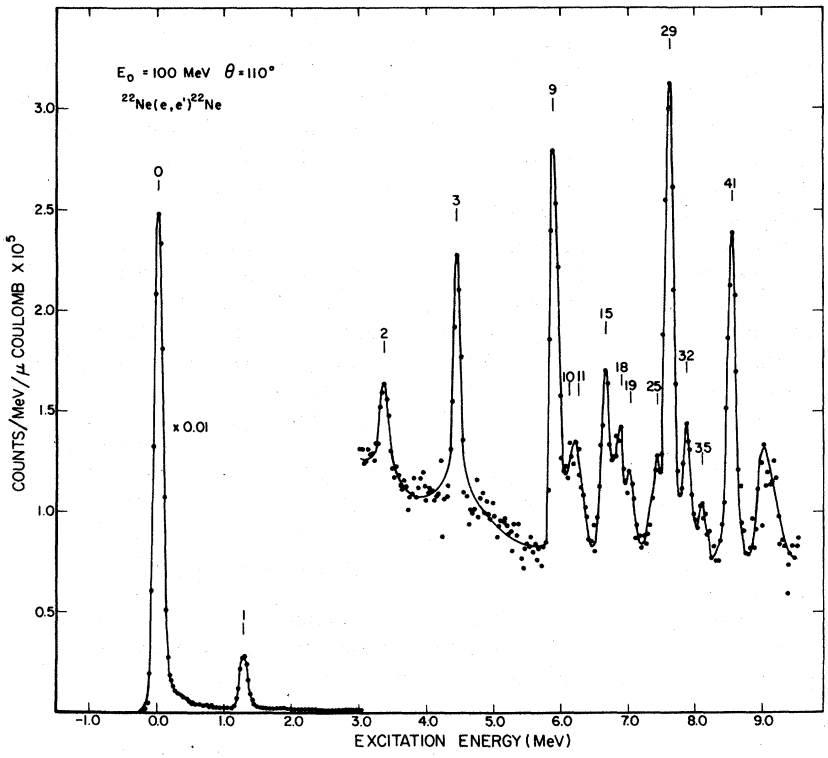

FIG. 1. Spectrum observed at $\theta = 110°$ from 100 MeV electrons incident on ^{22}Ne. The lines through the data are guides to the eye. Peak identification numbers correspond with those used in Table VIII.

TABLE II. Ratio of inelastic to elastic peak areas observed in this experiment.

E_0 (MeV)	θ (deg)	E_x (MeV) 1.275	3.36	$A_I/A_E \times 10^3$ 4.46	5.35	5.91
59.59	110.39	9.77 ± 0.24	≤0.15	0.487 ± 0.057	≤0.15	0.176 ± 0.049
59.59	110.39	11.01 ± 0.37	≤0.15	0.461 ± 0.048	≤0.015	0.187 ± 0.030
59.59	110.39	10.38 ± 0.17	≤0.15	0.525 ± 0.036	≤0.015	0.179 ± 0.033
69.69	110.45	19.72 ± 0.27	≤0.3	0.911 ± 0.048	0.103 ± 0.020	0.511 ± 0.037
69.91	110.39	23.17 ± 0.23	≤0.3	0.927 ± 0.064	≤0.3	0.492 ± 0.056
85.13	110.36	49.61 ± 0.63	0.264 ± 0.063	2.05 ± 0.08	≤0.3	2.027 ± 0.073
100.34	110.36	109.5 ± 1.4	1.75 ± 0.13	4.35 ± 0.17	≤0.5	7.36 ± 0.18
110.61	110.28	169.1 ± 2.1	4.1 ± 1.3	7.71 ± 0.30	≤0.8	16.72 ± 0.38
63.84	128.16	19.65 ± 0.60	≤0.4	0.778 ± 0.063	0.301 ± 0.051	...
77.42	128.17	46.88 ± 0.47	0.26 ± 0.15	1.92 ± 0.12	≤0.4	1.905 ± 0.070
110.56	128.05	311.6 ± 6.5	13.0 ± 1.5	13.22 ± 0.95	≤3.0	43.22 ± 1.06
		E_x (MeV) 6.14	6.27	6.70	6.90	7.06
59.59	110.39	0.187 ± 0.044	0.178 ± 0.044	0.211 ± 0.048	0.534 ± 0.053	...
59.59	110.39	0.106 ± 0.032	0.174 ± 0.033	0.191 ± 0.029	0.479 ± 0.029	...
59.59	110.39	0.115 ± 0.034	0.166 ± 0.038	0.128 ± 0.033	0.424 ± 0.043	0.117 ± 0.036
69.91	110.39	0.232 ± 0.069	0.280 ± 0.071	0.376 ± 0.055	0.823 ± 0.057	0.206 ± 0.056
85.13	110.36	0.488 ± 0.073	0.461 ± 0.076	0.941 ± 0.057	1.276 ± 0.059	0.359 ± 0.055
100.34	110.36	1.26 ± 0.19	1.29 ± 0.19	3.19 ± 0.16	2.16 ± 0.15	1.13 ± 0.14
110.61	110.28	2.16 ± 0.34	2.49 ± 0.34	5.90 ± 0.34	2.31 ± 0.32	1.79 ± 0.32
77.42	128.17	0.572 ± 0.070	0.628 ± 0.070	1.085 ± 0.063	1.706 ± 0.068	0.391 ± 0.049
110.56	128.05	4.34 ± 0.87	5.28 ± 0.88	14.14 ± 0.74	4.11 ± 0.91	3.44 ± 0.97
		E_x (MeV) 7.46	7.65	7.93	8.17	8.59
59.59	110.39	≤ 0.2	0.712 ± 0.049	0.159 ± 0.029	0.049 ± 0.027	0.356 ± 0.022
69.91	110.39	0.162 ± 0.031	1.550 ± 0.065	0.377 ± 0.051	≤ 0.2	0.831 ± 0.056
85.13	110.36	0.609 ± 0.056	4.122 ± 0.071	0.973 ± 0.059	0.377 ± 0.061	2.19 ± 0.15
100.34	110.36	2.06 ± 0.15	0.27 ± 0.20	2.00 ± 0.16	0.75 ± 0.16	6.06 ± 0.20
100.61	110.28	4.63 ± 0.31	16.60 ± 0.38	3.12 ± 0.30	1.94 ± 0.32	11.98 ± 0.35
77.42	128.17	0.634 ± 0.050	4.321 ± 0.063	0.885 ± 0.079	0.329 ± 0.071	2.54 ± 0.18
110.56	128.05	9.66 ± 0.73	34.74 ± 0.97	4.32 ± 0.68	3.96 ± 0.70	31.04 ± 1.05

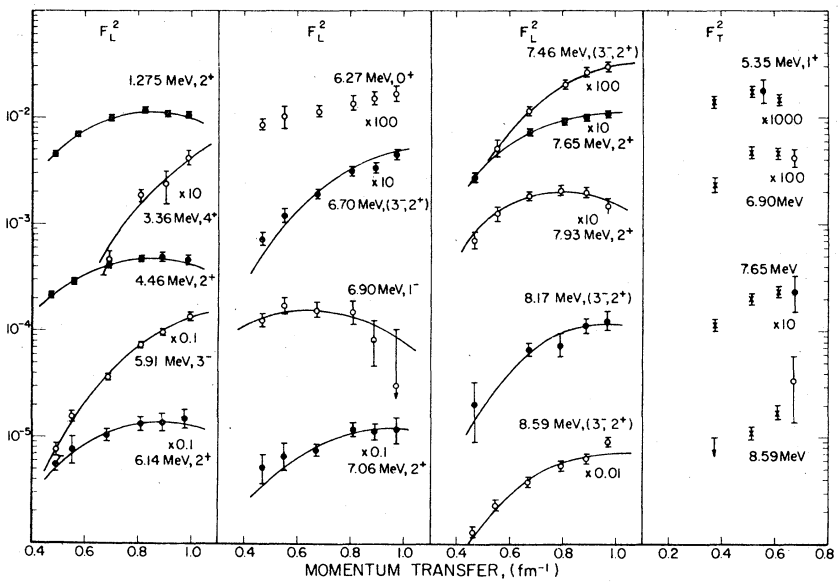

FIG. 2. Born approximation form factors for states observed in this experiment. F_L^2 for all states except at 6.27 MeV are the longitudinal squared form factors with Coulomb distortion corrections f_c applied. F_T^2 are the transverse squared form factors without Coulomb distortion corrections. The circles are measurements obtained in this experiment. Open and closed circles are used to aid in distinguishing among the various states. The solid line through the data are fits obtained using the generalized Helm model (model 4 of Table V). The crosses represent the 180° electron scattering data of Ref. 8.

TABLE III. Coulomb correction factors $f_c = \sigma$(Born approximation)/σ(distorted wave). Coulomb correction factors were calculated with the code by GBROW neglecting electron mass using a Fermi transition density with charge distribution parameters set equal to the elastic scattering values $c = 2.782$ and $t = 2.412$. For $C1$ and $C3$, an excitation energy of 7 MeV was assumed. The excitation energy for $C2$ was 1.275 MeV, and for $C4$, 3.36 MeV.

E_0 (MeV)	θ (deg)	$C1$	$C2$	$C3$	$C4$
59.59	110.39	0.962	0.894	0.859	···
69.69	110.45	0.990	0.913	0.874	···
69.91	110.39	0.990	0.913	0.874	···
85.13	110.36	1.044	0.954	0.909	0.867
100.34	110.36	1.119	0.996	0.936	0.868
110.61	110.28	1.183	1.031	0.933	0.894
63.84	128.16	···	0.909	···	···
77.42	128.17	1.044	0.948	0.897	0.822
110.56	128.05	1.299	1.081	0.987	0.918

may be written in the usual manner,

$$\left(\frac{d\sigma}{d\Omega}\right)_{\text{inel}} = \sigma_{\text{Mott}} F^2(q), \tag{3.2}$$

where

$$\sigma_{\text{Mott}} = \frac{Z^2 e^4}{4E_0^2} \frac{\cos^2(\frac{1}{2}\theta)}{\sin^4(\frac{1}{2}\theta)} \frac{1}{1+(2E_0/Mc^2)\sin^2(\frac{1}{2}\theta)}. \tag{3.3}$$

σ_{Mott} is the Mott cross section representing scattering from a point spinless nucleus of atomic number Z and mass M, E_0 is the incident electron energy, θ is the scattering angle, and q is the momentum transfer. The total form factor F consists of a longitudinal part F_L and a transverse part F_T defined as

$$F^2(q) = F_L^2(q) + [\tfrac{1}{2} + \tan^2(\tfrac{1}{2}\theta)] F_T^2(q). \tag{3.4}$$

In order to differentiate the contributions from the longitudinal and transverse form factors, cross sections were measured at 110° and 128°

TABLE IV. Squared longitudinal form factors, F_L^2 obtained from this experiment. Coulomb correction factors f_c have been applied to all states. For the state at 6.27 MeV, no Coulomb correction factor was applied. F_L^2 for the states at 6.70, 7.46, 8.17, and 8.59 MeV are tabulated assuming $J^\pi = 3^-$; to compute F_L^2 assuming $J^\pi = 2^+$ for these states, multiply by the ratio $f_c(2^+)/f_c(3^-)$ from the values of Table III.

			$F_L^2 \times 10^3$			
E_0 (MeV)	θ (deg)	E_x (MeV), J^π 1.275, 2^+	3.36, 4^+	4.46, 2^+	5.91, 3^-	6.14, 2^+
59.59	110.39	4.30 ± 0.21	···	0.215 ± 0.027	0.075 ± 0.021	0.083 ± 0.020
59.59	110.39	4.85 ± 0.26	···	0.204 ± 0.015	0.080 ± 0.013	0.047 ± 0.014
59.59	110.39	4.57 ± 0.20	···	0.232 ± 0.019	0.070 ± 0.023	0.051 ± 0.012
69.69	110.45	6.56 ± 0.28	···	0.304 ± 0.020	0.163 ± 0.013	···
69.91	110.39	7.68 ± 0.32	···	0.309 ± 0.025	0.157 ± 0.019	0.078 ± 0.023
85.13	110.36	9.89 ± 0.42	0.004 ± 0.011	0.430 ± 0.024	0.387 ± 0.021	0.098 ± 0.015
100.34	110.36	11.61 ± 0.49	0.163 ± 0.012	0.462 ± 0.026	0.736 ± 0.035	0.134 ± 0.021
110.61	110.28	10.86 ± 0.46	0.229 ± 0.075	0.496 ± 0.028	0.974 ± 0.045	0.139 ± 0.023
63.84	128.16	6.48 ± 0.33	···	0.257 ± 0.023	···	···
77.42	128.17	9.39 ± 0.39	0.045 ± 0.026	0.386 ± 0.029	0.362 ± 0.020	0.115 ± 0.015
110.56	128.05	10.84 ± 0.57	0.386 ± 0.045	0.461 ± 0.040	1.377 ± 0.075	0.151 ± 0.031
		E_x (MeV), J^π 6.27, 0^+	6.70, (3^-,2^+)	6.90, 1^-	7.06, 2^+	7.46, (3^-,2^+)
59.59	110.39	0.089 ± 0.022	0.090 ± 0.021	0.156 ± 0.030	···	···
59.59	110.39	0.087 ± 0.016	0.082 ± 0.013	0.130 ± 0.020	···	···
59.59	110.39	0.083 ± 0.019	0.055 ± 0.014	0.103 ± 0.025	0.052 ± 0.016	···
69.91	110.39	0.102 ± 0.026	0.121 ± 0.018	0.175 ± 0.028	0.068 ± 0.019	0.052 ± 0.010
85.13	110.36	0.097 ± 0.016	0.180 ± 0.013	0.164 ± 0.021	0.072 ± 0.011	0.116 ± 0.012
110.34	110.36	0.138 ± 0.020	0.319 ± 0.021	0.152 ± 0.037	0.120 ± 0.016	0.206 ± 0.017
110.61	110.28	0.156 ± 0.021	0.344 ± 0.024	0.083 ± 0.042	0.115 ± 0.021	0.271 ± 0.021
77.42	128.17	0.133 ± 0.015	0.207 ± 0.015	0.165 ± 0.043	0.079 ± 0.010	0.121 ± 0.011
110.56	128.05	0.170 ± 0.028	0.451 ± 0.032	0.031 ± 0.073	0.120 ± 0.034	0.308 ± 0.028
		E_x (MeV), J^π 7.65, 2^+	7.93, 2^+	8.17, (3^-,2^+)	8.59, (3^-,2^+)	
59.59	110.39	0.282 ± 0.025	0.072 ± 0.013	0.021 ± 0.012	0.131 ± 0.012	
69.91	110.39	0.467 ± 0.030	0.127 ± 0.018	···	0.235 ± 0.021	
85.13	110.36	0.762 ± 0.038	0.195 ± 0.014	0.074 ± 0.012	0.371 ± 0.034	
100.34	110.36	0.921 ± 0.049	0.213 ± 0.019	0.075 ± 0.016	0.557 ± 0.034	
110.61	110.28	1.007 ± 0.053	0.201 ± 0.021	0.113 ± 0.019	0.653 ± 0.037	
77.42	128.17	0.751 ± 0.045	0.179 ± 0.018	0.063 ± 0.014	0.396 ± 0.042	
110.56	128.05	1.122 ± 0.073	0.151 ± 0.025	0.126 ± 0.023	0.917 ± 0.064	

with the same momentum transfer, $q = 0.70$ fm^{-1}, and a Rosenbluth plot of the squared form factor versus $\frac{1}{2}+\tan^2(\frac{1}{2}\theta)$ was obtained. The choice of scattering angles for a longitudinal-transverse separation of the scattering cross section was restricted by the gas target cell geometry.

Peaks observed at excitation energies of 5.35, 6.90, 7.65, and 8.59 MeV exhibited non-negligible transverse cross sections. Figure 2 shows the transverse squared form factors obtained from the present experiment compared with the squared form factors from the 180° (e, e') experiment[8] done at the Naval Research Laboratory. The two experiments are in agreement as to the magnitude of the transverse electron scattering form factors. We therefore have assumed that the transverse form factors are represented by a smooth function passing through the 180° (e, e') data, but no assumptions as to the multipolarity of the transitions have been made. The contributions from the transverse cross sections were then subtracted from the total cross section and the squared longitudinal form factors were obtained. The other states in the spectrum had transverse form factors too small to measure, so for these states the subsequent analysis neglected the transverse contributions to the cross section.

The limited range of momentum transfers did not warrant a complete distorted-wave Born approximation (DWBA) treatment. Instead, correction factors $f_c = \sigma$(Born approximation)/σ(distorted wave) were applied to the longitudinal squared form factors in order to account for Coulomb distortion effects and the resultant equivalent Born form factors were analyzed in the Born approximation. These factors f_c were computed using the inelastic distorted wave code GBROW[14] with electron mass equal to zero for computational facility. The ground state Fermi charge distribution in a Tassie model was used to compute these correction factors for all multipolarities. Since the values of f_c do not deviate substantially from unity ($|f_c - 1| \leq 0.3$) and are not particularly sensitive to the nuclear model, more sophisticated corrections were deemed not to be warranted. Table III presents values for f_c used in this work. For the proposed 0^+ state at 6.27 MeV the analysis has been done in the simple Born approximation, as reliable values for f_c for 0^+ transitions were not available.

Table IV gives the squared longitudinal form factors in the Born approximation resulting from this analysis. Figure 2 presents the squared longitudinal Born approximation form factors for the states observed in ^{22}Ne. The form factors for $C1$, $C2$, $C3$, and $C4$ transitions exhibit substantially different momentum transfer dependence. The shape of the 6.90 MeV state form factor is characteristic of a $C1$ transition, the 1.275, 4.46, 6.14, 6.27, and 7.65 MeV form factors of $C2$, the 5.91 MeV form factor of $C3$, and the 3.36 MeV form factor of $C4$. The states at 6.70, 7.46, 8.17, and 8.59 MeV have form factors with similar momentum transfer dependence which are intermediate between the q dependence for the known $C2$ form factor of the 1.275 MeV state and the $C3$ form factor of the 5.91 MeV state. As the states in question could have transition charge densities more complicated than can be obtained from collective models, we cannot rule out the possibility that we are observing either $C2$ or $C3$ transitions. In the case of ^{20}Ne, such a situation occurs for the form factors of the 7.84 and 7.43 MeV 2^+ states where the 7.43 MeV form factor exhibits $C4$ dependence and has been described as anomalous.[15] The $C0$ and "normal" $C2$ form factor shapes are similar at these momentum transfers, so definite assignments for the 0^+ and 2^+ states require additional information from other experiments.

The spin and parity of the observed states were deduced from a comparison of experimental and calculated momentum transfer dependence of the longitudinal form factors. The J^π assignments will be discussed in more detail in the next section.

The squared longitudinal form factors were fitted in a model dependent manner to extract the reduced transition probabilities $B(CL)\uparrow$. In extracting electromagnetic transition strengths, the largest uncertainty arises from model dependence. We have extracted the reduced transition probabilities using six model dependent procedures in order to investigate the sensitivity of the strengths to variations in model parameters. The $F_L^2(q)$ were fitted using a Tassie model[16] with a Fermi ground state charge distribution and using a generalized Helm model.[17] For the Tassie model, the reduced transition probabilities were fitted with c and t fixed to ground state values and then with c and t individually allowed to vary. In the generalized Helm model, the reduced transition probabilities were obtained by fitting the strength parameter β, first with R and g allowed to vary, then with R and g fixed to the ground state value, and finally with only g fixed to the ground state value. Table V presents the reduced transition probabilities obtained from these six procedures. The average values of $B(CL)\uparrow$ obtained from the fitting procedures are given in Table VI. The uncertainties reflect the range of $B(CL)\uparrow$ including fitting errors allowed by the models investigated.

The scattering angles employed in this exper-

TABLE V. Reduced transition probabilities $B(CL)\uparrow$ obtained from fitting the (e,e') squared longitudinal form factors with various model assumptions. Models 1–3 use the Fermi charge distribution in a Tassie model. Model 1 fixes c and t, model 2 fixes t, and model 3 fixes c to the values obtained from elastic scattering. Models 4–6 use the generalized Helm model. Model 5 fixes g and R and model 6 fixes g to the elastic scattering parameter values. Model 4 allows g and R to vary. * indicates that satisfactory fits could not be made with the model assumptions.

		$B(CL)\uparrow$ (e^2fm^{2L})					
E_x (MeV)	J^π	1	2	3	4	5	6
1.28	2^+	284	273	270	270	*	256
3.36	4^+	*	*	17 200	16 200	17 500	17 000
4.46	2^+	12.7	13.2	13.4	13.3	*	12.4
5.91	3^-	*	970	850	840	850	822
6.14	2^+	3.5	3.2	3.3	3.2	2.7	3.0
6.70	2^+	*	4.0	3.2	3.2	5.7	3.2
	3^-	640	790	870	777	*	696
6.90	1^-	0.091	0.078	0.075	0.073	0.089	0.076
7.06	2^+	2.6	2.1	1.9	2.0	2.0	1.9
7.46	2^+	*	*	*	1.5	*	1.6
	3^-	430	360	360	347	241	332
7.65	2^+	*	18.8	17.9	18.1	18.5	17.5
7.93	2^+	5.5	6.5	6.6	5.6	4.1	6.0
8.17	2^+	*	1.4	1.3	1.3	*	1.3
	3^-	190	280	330	281	*	244
8.59	2^+	*	*	7	7	*	7
	3^-	*	*	*	*	*	1700

iment did not permit the extraction of much data on the transverse form factors. Four observed peaks at 5.35, 6.90, 7.65, and 8.59 MeV have transverse cross sections as exhibited in their Rosenbluth plots. A careful measurement of the cross section at 5.35 MeV was made to check for a longitudinal contribution. A Rosenbluth plot of the form factor obtained at $q = 0.56$ fm^{-1} is consistent with a purely transverse excitation and thus agrees with the observation of a

TABLE VI. Excitation energies and reduced transition probabilities. The energies of states from the literature identified with the experimentally observed states are presented along with the assumed J^π and deduced $B(CL)\uparrow$. The $B(CL)\uparrow$ are averages of those in Table V. The uncertainties associated with $B(CL)\uparrow$ reflect the range of values including fitting errors allowed by the models considered. Where fewer than four of the models considered allowed a satisfactory fit, the uncertainties are not presented. The reduced transition probabilities for those states are to be considered approximate values.

No.	E_x (lit.) (keV)	E_x (expt.) (MeV)	J^π	$B(CL)\uparrow$ (e^2fm^{2L})
1	1274.57 ± 0.02	1.275 ± 0.010	2^+	271 ± 36
2	3357.2 ± 0.4	3.36 ± 0.02	4^+	17 000 ± 4000
3	4456.7 ± 1.6	4.46 ± 0.02	2^+	13 ± 2
9	5909.9 ± 1.8	5.91 ± 0.02	3^-	870 ± 250
10	6115 ± 6	6.14 ± 0.04	2^+	3.2 ± 1.5
11	6237 ± 5	6.27 ± 0.05	0^+	3.8 ± 1.1
15	6691 ± 4	6.70 ± 0.02	2^+	3.9 ± 1.5
			3^-	750 ± 400
18	6904 ± 1.6	6.90 ± 0.03	1^-	0.08 ± 0.04
19	7052 ± 7	7.06 ± 0.03	2^+	2.1 ± 1.2
25	7470 ± 20	7.46 ± 0.03	2^+	1.6
			3^-	350 ± 250
29	7644 ± 4	7.65 ± 0.02	2^+	18 ± 3
32	7924 ± 6	7.93 ± 0.02	2^+	5.7 ± 2.4
35	8162 ± 4	8.17 ± 0.02	2^+	1.3 ± 1.3
			3^-	270 ± 270
41	8593 ± 7	8.59 ± 0.02	2^+	7
			3^-	1700

TABLE VII. Transverse squared form factors F_T^2 obtained from Rosenbluth plots of the total squared form factor obtained at electron scattering angles of 110° and 128°. Coulomb correction factors f_c have not been applied in obtaining F_T^2.

		$F_T^2 \times 10^3$		
q (fm^{-1})	E_x (MeV) 5.35	6.90	7.65	8.59
0.56	0.018 ± 0.003			
0.68		0.043 ± 0.008	0.024 ± 0.009	0.036 ± 0.022

magnetic dipole state in the NRL 180° electron scattering experiment.[8] Table VII tabulates the transverse form factors measured in this experiment.

The other three peaks with transverse strength have large longitudinal contributions. In the NRL 180° (e, e') experiment with an energy resolution of 250 keV (FWHM), states were observed at 6.82, 7.63, and 8.51 MeV whose squared transverse form factors are compatible with what is seen near those energies in the present experiment. Analysis of the previous experiment assumed that these states were magnetic, but the presence of longitudinal cross section in the present experiment suggests that more than a single state is being excited near each of these three energies. The results of the fitting procedure used in the present analysis give apparent peak position shifts of 40, 20, and 30 keV, respectively, for the 6.90, 7.65, and 8.59 MeV peaks as the momentum transfer is increased in this experiment. If the transverse cross section were to be associated with the state giving rise to the longitudinal cross section, a fit of $[B(EL, q)]^{1/2}$ and $[B(CL, q)]^{1/2}$ as polynomial functions of the squared momentum transfer gives electric and Coulomb reduced transition probabilities incompatible with each other in the context of Siegert's theorem, i.e., for the state at 6.90 MeV, $B(E1) > 10B(C1)$, at 7.65 MeV, $B(E2) > 5B(C2)$, and at 8.59 MeV, $B(E3) > 4B(C3)$. There are large uncertainties associated with the extrapolated reduced transition probabilities, and the possibilities for spin flip contribution[18] to electric transverse form factors have not been considered. These considerations and the complicated level structure of ^{22}Ne make it difficult to identify the longitudinal and transverse cross sections as arising from the excitation of the same state.

IV. DISCUSSION

The level scheme of ^{22}Ne presented in Table VIII contains over 40 states in the energy region of interest in this experiment. Below 6.35 MeV, there are 13 states whose spin and parity are generally considered to be established. Above 6.35 MeV, there are still uncertainties as to J^π assignments. Table VIII gives the level scheme obtained from recent experiments, the compilations[5,6] of Endt and Van der Leun, as well as that adopted for this study. The states marked with * have adopted J^π values influenced or confirmed by electron scattering data and those with † are other states whose J^π assignments have been modified or made more certain since the 1973 Endt and Van der Leun compilation.[5]

In analyzing the electron scattering data, the assumption is made that the electrons have not excited any states which have not been previously observed with other reaction mechanisms. It is further assumed that the observed form factors are due to single states. The possibility cannot, however, be ruled out that in certain cases unresolved states with differing multipolarities may be excited, giving rise to an apparently unique, but incorrect, form factor multipolarity signature. The excitation energies observed in this experiment are presented in Table VI along with excitation energies of states in the literature with which we identify the electron scattering peaks. We discuss below each of the states observed in this experiment and make comparisons with other experimental observations.

1.275 MeV. There is now considerable experimental information concerning the properties of the first excited state in ^{22}Ne. The excitation energy of the 2_1^+ state has been extremely well determined by a β^+ decay measurement[6] to be 1274.57 ± 0.02 keV. Transition strengths have been obtained from lifetime measurements using the Doppler shift attenuation and recoil distance methods, and from Coulomb excitation experiments, as well as from electron scattering. Although there have been compilations which have averaged the results of these measurements, as has been noted by Olsen *et al.*,[19] many of the earlier experiments had insufficient accuracy compared to more recent measurements. In recent experiments, the recoil distance method

TABLE VIII. Excitation energies (keV) and spin and parity information from selected recent works. The states marked with * have adopted J^π values influenced or confirmed by electron scattering data and those with † are other states whose J^π assignments have been modified or made more certain since the 1973 Endt–Van der Leun compilation.

No.	E_x (keV) [a]	1973 [b]	$(\alpha,p\gamma)$ [c]	$(\alpha,p\gamma)$ [d]	$(^7\text{Li},t\gamma)$ [e]	$(^6\text{Li},d)$ [f]	180° (e,e') [g]	Present (e,e')	1977 [h]	Adopted
1	1274.57 ± 0.02	2^+	2^+	2^+	2^+	2^+		2^+	2^+	2^+
2	3357.2 ± 0.4	4^+	4^+	4^+	4^+	4^+		4^+	4^+	4^+
3	4456.7 ± 1.6	2^+	2^+	2^+	2^+	2^+		2^+	2^+	2^+
4	5147.5 ± 1.7	2^-							2^-	2^-
5	5336 ± 5	$(1,2)^+$			1^+	1^+	1^+	1^+	1^+	1^+*
6	5365 ± 2	2^+		2^+	2^+	2^+			2^+	2^+
7	5523.2 ± 0.6	4^+	2,3,4	4^+		4^+			4^+	4^+
8	5641.3 ± 0.7	3^+	2,3	3^+					3^+	3^+
9	5909.9 ± 1.8	2^+	1,3	2^+		3^-		3^-	3^-	3^-*
10	6115 ± 6	π^{nat}	1,2,3	2^+	2^+			2^+	2^+	2^+*
11	6237 ± 5	π^{nat}				0^+		$(0,2)^+$	0^+	0^+*
12	6311.4 ± 1.7		6	6^+		6^+			6^+	6^+†
13	6345.2 ± 0.9	6^+		4^+		4^+			4^+	4^+†
14	6636.0 ± 1.7	$(0-4)^+$		$2^+,3^+$					$(2,3)^+$	$(2,3)^+$†
15	6691 ± 4	π^{nat}		1^-				$(3^-,2^+)$	1^-	$(3^-,2^+)$*
16	6817 ± 2	2^+	1,2	2^+					2^+	2^+
17	6849 ± 2	$(1,2)^+$		1^+			1^+		1^+	1^+*
18	6904 ± 9			(0^+)				1^-	$(0,1)^+$	(1^-)*
19	7052 ± 7	$(1,3)^-$	0,1,2					2^+	1^-	2^+*
20	7341.1 ± 1.1	$(0,2,4)^+$	3,4	(3^+)					$(3,4)^+$	(3^+)†
21	7342 ± 6				(0^+)	0^+			0^+	(0^+)†
22	7350 ± 20									(1^-)
23	7406 ± 2	$(1,3)^-$	3,5	$(1,3)^-$				$(3^-,2^+)$	$(1,3)^-$	(3^-)*
24	7423.0 ± 0.8			(5^+)					$(3,5)^+$	(5^+)†
25	7470 ± 20							$(3^-,2^+)$		$(3^-,2^+)$*
26	7489 ± 6	$(1,3)^-$			1^-				1^-	
27	7500 ± 20									
28	7537 ± 5	$(4,5)^+$								$(4,5)^+$
29	7644 ± 4	$(1,2)^+$			2^+	2^+		2^+	2^+	2^+*
30	7664 ± 8	$(0-3)^-$					2^-		2^-	2^-*
31	7721 ± 3	$(1,3)^-$	2,3,4	3^-	3^-	3^-			3^-	3^-†
32	7924 ± 6	2^+			2^+			2^+	2^+	2^+*
33	8081 ± 4	$(0-4)^+$							$(2-4)^+$	$(0-4)^+$
34	8131 ± 7				2^+	2^+			2^+	2^+†
35	8162 ± 4		3					$(3^-,2^+)$	3^-	3^-*
36	8382 ± 7	π^{nat}	3,4						$(3^-,4^-)$	$(3^-,4^-)$†
37	8491 ± 2	$(1,2)^+$	5						2^+	
38	8549 ± 2	$(0-4)^+$					2^-		$(0-4)^+$	
39	8575 ± 7				1^-					1^-†
40	8585 ± 7	$(1,2)^+$			(2^+)					
41	8593 ± 7				$(3^-,4^+,5^-)$			$(3^-,2^+)$		(3^-)*
42	8737 ± 7	$(0-3)^-$							3^-	3^-
43	8861 ± 4								$(0-4)^+$	+†

[a] Excitation energies from 1978 compilation, Ref. 6, except states 17, 22, 27, 28, 38–41; states 39–41 from Ref. 2; states 17, 38 from Ref. 32; states 22, 27, 28 from 1973 compilation, Ref. 5.
[b] 1973 compilation, Ref. 5.
[c] ^{19}F$(\alpha,p\gamma)^{22}$Ne, Ref. 3.
[d] ^{19}F$(\alpha,p\gamma)^{22}$Ne, Ref. 2.
[e] ^{18}O$(^7\text{Li},t\gamma)^{22}$Ne, Ref. 2.
[f] ^{18}O$(^6\text{Li},\alpha)^{22}$Ne, Ref. 34.
[g] ^{22}Ne$(e,e')^{22}$Ne, Ref. 8.
[h] 1978 compilation, Ref. 6.

used by Anyas-Weise *et al.*,[20] Horstmann *et al.*,[21] and Radford and Poletti[22] gives the results $\tau = 5.4 \pm 0.4$, 5.2 ± 0.3, and 5.6 ± 0.2 ps corresponding to $B(C2)\uparrow = 224 \pm 17$, 233 ± 13, and 216 ± 8 e^2 fm^4, respectively. The Coulomb excitation experiment of Olsen *et al.*[19] yielded $B(C2)\uparrow = 224 \pm 17$ e^2 fm^4 and the electron scattering experiment of Singhal *et al.*[7] gave a value of 220 ± 20 e^2 fm^4. The present value of 271 ± 36 e^2 fm^4 is in agreement with the previous values. Table IX lists lifetimes, reduced transition probabilities, and transition strengths obtained from the literature and from

TABLE IX. Lifetimes, reduced matrix elements, and transition strengths for the 1.275 MeV 2^+ state obtained from the literature and the present experiment. DSAM is Doppler shift attenuation method, RD is recoil distance method, CE is Coulomb excitation, and ES is electron scattering. The measurements are lifetime for DSAM and RD, whereas CE and ES measure the reduced matrix element $B(C2)\uparrow$.

τ (ps)	$B(C2)\uparrow$ (e^2 fm^4)	$\lvert M\rvert^2$ (Weisskopf units)	Method	Ref.
$6.1^{+4.6}_{-2.6}$	193^{+143}_{-82}	$10.5^{+7.8}_{-4.5}$	DSAM	27
8 ± 3	150 ± 60	8 ± 3	DSAM	35
4.6 ± 0.5	263 ± 29	14.4 ± 1.6	RD	36
2 – 10			RD	37
6.1 ± 0.5	198 ± 16	10.9 ± 0.8	RD	38
5.9 ± 1.1	205 ± 38	11.2 ± 2.1	RD	39
5.9 ± 0.6	205 ± 21	11.2 ± 1.1	RD	40
5.4 ± 0.4	224 ± 17	12.2 ± 0.9	RD	20
5.6 ± 0.2	216 ± 8	11.8 ± 0.4	RD	22
5.2 ± 0.3	233 ± 13	12.7 ± 0.7	RD	21
3.1 ± 1.1	390 ± 140	21.3 ± 7.5	CE	41
3.7 ± 0.7	330 ± 60	18.0 ± 3.3	CE	42
4.7 ± 0.5	260 ± 20	14.2 ± 1.4	CE	43
4.8 ± 0.4	250 ± 20	13.7 ± 1.1	CE	19
5.5 ± 0.3	220 ± 20	12.0 ± 1.1	ES	7
4.6 ± 0.6	271 ± 36	14.9 ± 2.0	ES	present

the present experiment. The present experimental value for $B(C2)\uparrow$ results in a lifetime of $\tau = 4.5 \pm 0.6$ ps and, in the adiabatic rotational model, the quadrupole moment of the intrinsic state of the $K = 0$ band is $Q_0 = 52 \pm 4$ e^2 fm^2 (obtained from the formula[23] $Q_0 = [16\pi B(C2)\uparrow/5]^{1/2}$).

Although there is apparent agreement between the present value for $B(C2)$ and the value obtained by the Saskatchewan electron scattering group,[7] this is only because of the relatively large model dependent uncertainty quoted in the present experiment. The analysis of the present data using the aforementioned Tassie and generalized Helm models with all parameters allowed to vary gives $B(C2)\uparrow = 279 \pm 24$ and 270 ± 20 e^2 fm^4, respectively, which is to be compared to the value $B(C2)\uparrow = 220 \pm 20$ e^2 fm^4 obtained by Singhal *et al.*[7] using the same models. This difference is somewhat difficult to reconcile, since the same elastic cross section parameters were used in analyzing both experiments and the ratio of inelastic to elastic cross sections was measured in both cases.

3.36 MeV. The 4^+ state at 3357.2 ± 0.4 keV has a lifetime[24] of 324 ± 9 fs. The present experimental result for the reduced transition probability of $B(C4)\uparrow = 17\,000 \pm 4000$ e^2 fm^8 confirms the previous observation that the branching ratio is nearly 100% to the 2_1^+ state.[25] The lifetime measurement by Alexander *et al.*[24] is in agreement with the measurement of Fifield *et al.*[26]

4.46 MeV. The present experiment yields $B(C2)\uparrow = 13.0 \pm 2$ e^2 fm^4 for the 2_2^+ state at 4456.7 ± 1.6 keV. Using the value for the branching ratio to the ground state obtained by Kutschera *et al.*,[25] $\gamma_0/\Gamma = (3 \pm 2)\%$, the lifetime is 5 ± 4 fs, consistent with the latest upper limit determination of 15 fs. This upper limit value obtained from a Doppler shift attenuation method experiment of Alexander *et al.*[24] supersedes several previous measurements.[25,27,28]

5.35 MeV. There are two states, at 5336 ± 5 and 5365 ± 2 keV, which could be identified with the peak seen in the present experiment. The spin and parity of the state at 5.365 MeV was determined to be $J^\pi = 2^+$ on the basis of angular distribution studies of the ^{21}Ne$(d,p)^{22}$Ne reaction.[4] The other member of the doublet at 5.336 MeV was determined to have either spin 1 or 2 in the same study, and its absence in the ^{18}O$(^7$Li$,t)^{22}$Ne study[1] strongly suggested unnatural parity, favoring $J^\pi = 1^+$. The ^{20}Ne$(t,p\gamma)^{22}$Ne angular correlation study by Howard *et al.*[29] determined its spin to be 1. Subsequently, Maruyama *et al.*[8] observed the same state in a $180°(e,e')$ experiment and from the momentum transfer dependence of the form factor confirmed the spin and parity assignment to be $J^\pi = 1^+$. In the present experiment a careful measurement at scattering angles of 110° and 128° with $q = 0.56$ fm^{-1} establishes the transverse character of the observed transition and thus is identified with the 5.336 MeV 1^+ state. The present experiment is not favorable to the study of magnetic transitions, so extraction of $B(M1)\uparrow$ values was not attempted. However, the measurement to confirm the magnetic character of the observed state is, as already noted, in agreement with the 180° (e,e') study. The reduced matrix element from that work is $B(M1)\uparrow = 0.444 \pm 0.078\mu_0^2$. Using the branching ratios[2] $\gamma_0/\Gamma = 0.69 \pm 0.06$ and $\gamma_1/\Gamma = 0.31$

± 0.06, the deduced total width of the 1^+ state is $\Gamma = 0.38 \pm 0.07$ eV, corresponding to a mean life $\tau = 1.7 \pm 0.3$ fs.

5.91 MeV. The state at 5909.9 ± 1.8 keV has been reported to have $J^\pi = 2^+$. However, the recent ^{19}F$(\alpha, p\gamma)^{22}$Ne angular correlation measurement of Broude *et al.*[3] together with information existing on the population of this level in the ^{20}Ne$(t, p\gamma)^{22}$Ne and ^{22}Ne$(\alpha, \alpha')^{22}$Ne reactions[29,30] give strong evidence that $J^\pi = 3^-$. The (e, e') form factor confirms the 3^- spin and parity assignment. The present analysis gives $B(C3)\uparrow = 870 \pm 250\ e^2\,\mathrm{fm}^6$.

6.14 MeV. The state at 6115 ± 6 keV is identified as having spin and parity $J^\pi = 2^+$ from the work of Howard *et al.*[29] and Flynn *et al.*,[31] with γ-ray branching ratios of (14 ± 2), (78 ± 3), and (8 ± 1)% to the ground, 2_1^+, and 2_2^+ states, respectively. In contrast, Broude *et al.*[3] in their $(\alpha, p\gamma)$ study find branching ratios of (90 ± 5) and (10 ± 5)% to the 2_1^+ and 2_2^+ states, respectively, with no direct decay to the ground state. The (e, e') analysis confirms $J^\pi = 2^+$ with $B(C2)\uparrow = 3.2 \pm 1.5\ e^2\,\mathrm{fm}^4$ corresponding to $\gamma_0 = (4.4 \pm 1.4) \times 10^{-3}$ eV, which confirms the existence of a ground state decay branch. If the branching ratio reported by Howard *et al.*[29] is used, the lifetime of this state is 21 ± 10 fs.

6.27 MeV. The structure observed at this approximate energy has a momentum transfer dependence of the form factor which is similar to that for states with $J^\pi = 2^+$. In electron scattering the 0^+ and 2^+ form factors have similar shapes, so definitive identification is not possible from the electron scattering data alone. There exist known states of $J^\pi = 0^+$ at 6237 ± 5 keV, 6^+ at 6311.4 ± 1.7 keV, and 4^+ at 6345.2 ± 0.9 keV. The electron spectra show a peak whose location shifts about 100 keV as the momentum transfer is increased. A reasonable interpretation of the measured form factor is that we are observing the excitation of the 0^+ state, with possibly some contribution from the 4^+ state at higher momentum transfers. If the state is identified with the 0^+ state, the matrix element is 3.8 ± 1.1 fm^2 obtained from fitting $[B(C0, q)]^{1/2}$ as a polynomial function in q^2.

6.70 MeV. Possible candidates for identification with this state occur at 6636.0 ± 1.7 and 6691 ± 4 keV. The 6.69 MeV γ decay angular correlation measured in the ^{19}F$(\alpha, p\gamma)^{22}$Ne reaction[2] indicates the higher excitation state to be $J = 1$, and its observation in the α scattering experiment of Ollerhead *et al.*[30] indicates natural parity. The results of ^{21}Ne$(d, p)^{22}$Ne and ^{19}F$(\alpha, p\gamma)^{22}$Ne studies[4,31] indicate that the lower energy member of this doublet has positive parity with spin 2 or 3. As discussed above, the form factor of the state observed in this experiment can be fitted with the assumption $J^\pi = 2^+$ or 3^-. A conclusive identification of the observed state with the candidate states cannot be made, but because of the observed excitation energy and because the $(\alpha, p\gamma)$ reaction[31] detected direct ground state γ decay radiation, tentative identification of this state with that observed at 6691 keV is made. A satisfactory reconciliation of the present results and the $(\alpha, p\gamma)$ angular correlation findings remains to be made. Assuming $J^\pi = 3^-$, $B(C3)\uparrow = 750 \pm 400\ e^2\,\mathrm{fm}^6$; assuming $J^\pi = 2^+$, $B(C2)\uparrow = 3.9 \pm 1.5\ e^2\,\mathrm{fm}^4$. The fitted curve in Fig. 2 assumes the transition is $C3$.

6.90 MeV. There are two states at 6849 ± 2 and 6904 ± 9 keV which are candidates for identification with the state observed in the present (e, e') experiment. The 6.85 MeV state has $J^\pi = 1^+$ as established by the angular correlation study of Fifield *et al.*[2] and the observation of $l_n = 0$ transfer in the ^{21}Ne$(d, p)^{22}$Ne experiment.[4] The 180° (e, e') study confirms the 1^+ spin and parity for a state in this region. As suggested above, the longitudinal and transverse form factors can arise from excitation of different states. The state at 6904 ± 9 keV has been observed with ^{18}O$(^7$Li$, t)^{22}$Ne and ^{20}Ne$(t, p)^{22}$Ne reactions.[1,2,31] It has been proposed that this state has $J^\pi = 0^+$ on the basis of the strongly forward peaked angular distribution observed in the α transfer reaction.[2,31] However, the work of Fifield *et al.*[2] shows good fits to the angular correlation for spin values of 1 and 2, as well. The observation of the state in the ^{18}O$(^7$Li$, t)^{22}$Ne spectrum[2] indicates that the state has natural parity. The structure observed in the present experiment has a form factor characteristic of $J^\pi = 1^-$ which would be compatible with identification with the state at 6.90 MeV. The reduced transition probability is $B(C1)\uparrow = 0.08 \pm 0.04\ e^2\,\mathrm{fm}^2$ corresponding to a ground state radiation width $\gamma_0 = 9 \pm 5$ eV. In the recent inelastic photon scattering experiment of Berg,[32] the spectrum shows no state of significant strength at 6.90 MeV. If the state observed in the present experiment is indeed electric dipole, it has sufficiently large ground state radiative width to allow it to be seen with resonance fluorescence. Consequently, the spin and parity assignment is tentative and the possibility of misidentification due to model errors cannot be ruled out.

7.06 MeV. Angular distribution studies of the ^{18}O$(^7$Li$, t)^{22}$Ne, ^{21}Ne$(d, p)^{22}$Ne, and ^{20}Ne$(t, p)^{22}$Ne reactions[1,4,29] have previously assigned $J^\pi = 1^-$ to the state at 7052 ± 7 keV. The present work reveals a momentum transfer dependence of the form factor characteristic of $J^\pi = 2^+$ with $B(C2)\uparrow = 2.1 \pm 1.2\ e^2\,\mathrm{fm}^4$ in disagreement with previous

results. Lending support to the findings of this result are the consistency with $J=0$, 1, or 2 in $^{19}F(\alpha,p\gamma)^{22}Ne$ studies[3] and the lack of appreciable strength in the $^{22}Ne(\gamma,\gamma')^{22}Ne$ experiment of Berg.[32] The $(t,p\gamma)$ study of Howard *et al.*[29] presents branching ratios of $(9\pm1$ and $(91\pm1)\%$, whereas the $(\alpha,p\gamma)$ study of Broude *et al.*[3] shows (0 ± 5) and $(100\pm5)\%$ for the γ decay to the ground and 2^+ states, respectively.

7.46 MeV. The present (e,e') spectra show a peak which exhibits predominantly longitudinal cross section indicating a state of natural parity. Candidate states which may be identified with the state observed in the present experiment are at 7406 ± 2, 7423.0 ± 0.8, 7470 ± 20, and 7489 ± 6 keV. The ^{22}F β decay measurement of Davids *et al.*[33] determined the spin and parity of the 7.42 MeV state to be $J^\pi=(3,4,5)^+$, with a strong preference for 5^+. The 7.47 MeV level has been reported only in an earlier $^{23}Na(t,\alpha)^{22}Ne$ experiment,[5] but has not been reported in subsequent experiments. For the states at 7.41 and 7.49 MeV, the $l_n=1$ stripping pattern observed in the $^{21}Ne(d,p)^{22}Ne$ reaction[4] and the natural parity deduced from inelastic α particle scattering[30] limit the spin and parity for both states to 1^- or 3^-. Furthermore, for the 7.49 MeV state, the $^{20}Ne(\alpha,p\gamma)^{22}Ne$ ground state γ angular distribution observed by Howard *et al.*[29] found only $J=1$ would fit the data. The $^{18}O(^7Li,t\gamma)^{22}Ne$ angular correlation measurement of Fifield *et al.*,[2] also corroborated this finding, with $J^\pi=1^-$ and branching ratios of (57 ± 4), (22 ± 4), and $(21\pm3)\%$ to the ground. 2_1^+, and 2_2^+ states, respectively. On the other hand, the resonance fluorescence measurement of Berg,[32] which would be sensitive to detecting 1^- states, did not see appreciable strength near this energy. The present analysis allows $J^\pi=2^+$ or 3^- for this state with $B(C2)\uparrow=1.6\ e^2\,\mathrm{fm}^4$ and $B(C3)\uparrow=350\pm250\ e^2\,\mathrm{fm}^6$. However, assuming a quadrupole transition allows fits for only two of the six models considered, so $B(C2)\uparrow$ is considered only an approximate value and an uncertainty is not assigned. It is suggested that the observed peak contains contributions from two or more states because the fitted peak excitation energy shows a decrease of 50 keV from the lowest to the highest momentum transfers of this experiment and because of the difficulty in fitting the peak as $J^\pi=2^+$. The electron scattering results could be explained if the state at 7.41 MeV were being excited with $J^\pi=3^-$ together with the state at either 7.47 or 7.49 MeV. However, if the 7.49 MeV were being electroexcited, then it would be difficult to reconcile the present observation with the earlier findings of $J^\pi=1^-$ for that state. Further studies are needed to clarify the spin and parity assignemnts for states near 7.46 MeV excitation energy. The fitted curve in Fig. 2 is for a $C3$ transition.

7.65 MeV. In the present experiment a peak is observed at 7.65 MeV with transverse contribution to the cross section. The 180° (e,e') experiment[8] done at NRL reported a $J^\pi=2^-$ state at nearly the same energy which was identified with the 7664 ± 8 keV state. Their transverse cross sections were used to extract the longitudinal cross section from the present data. The longitudinal form factor exhibits $J^\pi=2^+$ behavior with $B(C2)\uparrow=18\pm3\ e^2\,\mathrm{fm}^4$. The analysis to separate the longitudinal and transverse cross sections suggests that at least two states are contributing to the cross section observed for electron scattering in this excitation region. If the longitudinal contribution is from excitation of the state at 7644 ± 4 keV, the J^π restriction to $(1,2)^+$ from the $l_n=0+2$ neutron transfer in the $^{21}Ne(d,p)^{22}Ne$ reaction[4] and to $J^\pi=2^+$ from the $^{18}O(^7Li,t)^{22}Ne$ study[2] is confirmed. It is to be noted that electron scattering does not resolve the 7.64 and 7.66 MeV states directly, but a reasonable interpretation of the cross sections from longitudinal and transverse components can be made by the assumption of electroexcitation of both members of the doublet.

7.93 MeV. Electroexcitation of the 7924 ± 6 keV state confirms the $J^\pi=2^+$ determination of several previous measurements.[6] The deduced reduced transition probability is $B(C2)\uparrow=5.7\pm2.4\ e^2\,\mathrm{fm}^4$.

8.17 MeV. The 1973 compilation of Endt and Van der Leun[5] lists a state at 8136 keV with $J^\pi=(0,2,4)^+$ whose spin and parity can be assigned to be $J^\pi=2^+$ on the basis of analysis of a proton angular distribution experiment in the $^{21}Ne(d,p)^{22}Ne$ reaction.[4] The $^{18}O(^7Li,d)$ reaction[34] supports $J^\pi=2^+$. However, a more recent $^{20}Ne(t,p)^{22}Ne$ study by Flynn *et al.*[31] showed that there is in fact a doublet in this region with a 2^+ state at 8125 ±10 keV, and a second state at 8163 ± 10 keV. In a $(\alpha,p\gamma)$ study Broude *et al.*[3] observed a state at 8.14 MeV whose spin was 3. The level observed in the present experiment has a form factor shape similar to those for states at 6.69, 7.46, and 8.59 MeV for which a definite choice between $J^\pi=3^-$ and 2^+ cannot be made. If $J^\pi=3^-$, $B(C3)\uparrow=270\pm270\ e^2\,\mathrm{fm}^6$, and if $J^\pi=2^+$, $B(C2)\uparrow=1.3\pm1.3\ e^2\,\mathrm{fm}^4$. The 100% uncertainties associated with the reduced transition probabilities suggest that this experiment has not resolved the doublet of Flynn *et al.*[31] Tentatively, because of the observed excitation energy, the peak observed in electron scattering is identified as predominantly the one at 8.16 MeV, and it is assumed that it is the same state as seen by Broude *et al.*[3] The fit

to the data shown in Fig. 2 assumes a $C3$ transition.

8.59 MeV. There are several states in this energy region which are candidates for identification with the peak observed in electron scattering. A state at 8548 ± 10 keV is observed in the ^{21}Ne$(d,p)^{22}$Ne reaction[4] and has been given a tentative J^π assignment of $(0-4)^+$. In addition, ^{20}Ne$(t,p)^{22}$Ne, ^{18}O$(^7$Li$,t)^{22}$Ne, and ^{19}F$(\alpha,p\gamma)^{22}$Ne reactions[1-4] all observe a state at 8583 keV. In the present experiment a peak with both longitudinal and transverse cross sections is observed. The 180° electron scattering experiment studied the transverse cross section and concluded that the structure was to be associated with the lower energy member of the multiplet at 8549 keV. The resonance fluorescence work of Berg[32] observed a state of probable spin $J=1$ at 8549 ± 2 keV which is in contrast to the $J^\pi=2^-$ assignment from the 180° (e,e') experiment. Furthermore, Fifield *et al.*[2] have given evidence that the state at 8.58 MeV is a multiplet of at least three states. Their ^{19}F$(\alpha,p\gamma)^{22}$Ne study of the γ-ray decay shows 16, 62, and 22% intensities to the ground, 2_1, and 4_1 states, respectively. In their analysis, the ground state decay strongly suggests angular correlation compatible with $J^\pi=1^-$; the 4_1^+ decay is compatible with $J=3$, 4, or 5, and the decay to the 2_1^+ is indicative of another state in the same energy region. The energies ascribed to the states in the multiplet by Fifield *et al.* are 8575 ± 7, 8593 ± 7, and 8585 ± 7 keV, respectively. It should be noted, however, that their analysis did not resolve these states directly.

The form factor for the longitudinal cross section peak observed in this experiment could only be fitted with a few of the model assumptions of this analysis. Thus only an approximate value for $B(CL)$ is presented without estimated uncertainties. $B(C3)\uparrow = 1700\ e^2\,\mathrm{fm}^6$ and $B(C2)\uparrow = 7\ e^2\,\mathrm{fm}^4$. The complicated level scheme proposed near 8.59 MeV makes interpretation of electron scattering data difficult and makes these assignments tentative.

V. CONCLUSION

The analysis of the electron scattering experiment presented in this paper has resulted in new information on the reduced transition probabilities for transitions from the ground to many of the excited states in ^{22}Ne below particle emission threshold. The actual excitation energies have been adopted from more precise measurements of energies and the cross sections observed in this experiment have been identified with previously observed states. Below 6.35 MeV, the excited state spin and parities are now considered to be well established. Table VI tabulates the energies, spins and parities, and reduced transition probabilities deduced from this experiment. Table X presents lifetime and branching ratios of several states obtained both from (e,e') analysis and from other experiments. The present experiment has used previous 180° electron scattering data to estimate transverse contributions to the electron scattering cross section. The resultant longitudinal cross sections give information concerning the electromagnetic transition strengths for natural parity states in ^{22}Ne. Because of the complicated energy level scheme, a discussion of detailed theoretical implications is beyond the scope of this work. It is hoped that the present results will aid in future microscopic model calculations.

TABLE X. Lifetimes deduced from combining the results of this experiment with previously measured ground state γ decay branching ratios.

E_x	J^π	τ (fs)	γ_0/Γ (%)	Ref.
4.46	2^+	5 ± 4	3 ± 2	25
5.35	1^+	1.7 ± 0.3	69 ± 6	2,8
6.14	2^+	21 ± 10	14 ± 2	29
7.65	2^+	1.1 ± 0.5	13 ± 5	2

We thank Professor P. M. Endt and Professor C. Van der Leun for providing us with their energy level compilation prior to publication. We wish to thank Dr. U. Berg for the results of and discussions concerning his resonance fluorescence experiment. FJK acknowledges the support of a National Research Council Postdoctoral Research Associateship during the performance of this work. This work was supported in part by the National Science Foundation.

*Present address: Science Applications, Inc., 8400 Westpark Drive, McLean, Va. 22101.
†Present address: Physics Department, UCLA, Los Angeles, Calif. 90024.
‡Present address: Link Division of The Singer Co., 11800 Tech Road, Silver Spring, Md. 20904.

[1] W. Scholtz, P. Neogy, K. Bethge, and R. Middleton, Phys. Rev. C 6, 893 (1972).
[2] L. K. Fifield, R. W. Zumuhle, D. P. Balamuth, and S. C. Tabor, Phys. Rev. C 13, 1515 (1976).

[3]C. Broude, W. G. Davies, J. S. Forster, and G. C. Ball, Phys. Rev. C 13, 1953 (1976).
[4]P. Neogy, R. Middleton, and W. Scholtz, Phys. Rev. C 6, 885 (1972).
[5]P. M. Endt and C. Van der Leun, Nucl. Phys. A 214, 1(1973).
[6]P. M. Endt and C. Van der Leun, Nucl. Phys. A310, 1 (1978).
[7]R. P. Singhal, H. S. Caplan, J. R. Moreira, and T. E. Drake, Can. J. Phys. 51, 2125 (1973).
[8]X. K. Maruyama, R. A. Lindgren, W. L. Bendel, E. C. Jones, Jr., and L. W. Fagg, Phys. Rev. C 10, 2257 (1974); 17, 856 (1978).
[9]J. W. Lightbody, Jr., S. Penner, S. P. Fivozinsky, P. L. Hallowell, and Hall Crannell, Phys. Rev. C 14, 952 (1976).
[10]H. Crannell, J. M. Finn, P. Hallowell, and J. T. O'Brien, Nucl. Instrum. 126, 543 (1975).
[11]J. Heisenberg (private communication).
[12]J. R. Moreira, R. P. Singhal, and H. S. Caplan, Can. J. Phys. 49, 1434 (1971).
[13]Phillip R. Bevington, *Data Reduction and Error Analysis for the Physical Sciences* (McGraw-Hill, New York, 1969) p. 200.
[14]S. T. Tuan, L. E. Wright, and D. S. Onley, Nucl. Instrum. Methods 60, 70 (1968).
[15]S. Mitsunobue and Y. Torizuka, Phys. Rev. Lett. 28, 920 (1972).
[16]L. J. Tassie, Aust. J. Phys. 9, 407 (1956); 11, 481 (1958).
[17]M. Rosen, R. Raphael, and H. Uberall, Phys. Rev. 163, 927 (1967).
[18]M. Tomaselli, L. Grunbaum, G. A. Beer, H. G. Clerc, and G. Wittwer, Phys. Lett. 27B, 579 (1969).
[19]D. K. Olsen, A. R. Barnett, S. F. Biagi, N. H. Merrill, and W. R. Phillips, Nucl. Phys. A 220, 541 (1974).
[20]N. Anyas-Weise, R. Griffith, N. A. Jelley, W. Randolph, J. Szuss, and T. K. Alexander, Nucl. Phys. A 201, 513 (1973).
[21]R. E. Horstmann, J. L. Eberhardt, P. C. Zahn, H. A. Doubt, and G. Van Middlekoop, Nucl. Phys. A 275, 237 (1977).
[22]R. C. Radford, and A. R. Poletti, Nucl. Phys. A 275, 141 (1977).
[23]Alan Christy and O. Hausser, Nucl. Data Tables II, 281 (1972).
[24]T. K. Alexander, J. S. Forster, G. C. Ball, W. G. Davies, and I. V. Mitchell, Chalk River Nuclear Laboratory, Atomic Energy of Canada, Ltd., Report No. 18, 1978 (unpublished).
[25]W. Kutschera, D. Pelte, and G. Schrieder, Nucl. Phys. A 111, 529 (1968).
[26]L. K. Fifield, J. Asher, and A. R. Poletti, J. Phys. G 4, L65 (1978).
[27]M. A. Eswaren and C. Broude, Can. J. Phys. 42, 1311 (1964).
[28]E. K. Warburton, J. W. Olness, and A. R. Poletti, Phys. Rev. 160, 938 (1967).
[29]A. J. Howard, R. G. Hirko, D. A. Bromley, K. Bethge, and J. W. Olness, Nuovo Cimento 2A, 575 (1972).
[30]R. W. Ollerhead, G. F. R. Allen, A. M. Baxter, B. W. J. Gillespie, and J. A. Kuehner, Can. J. Phys. 49, 594 (1971).
[31]E. R. Flynn, O. Hansen, and O. Nathan, Nucl. Phys. A 228, 189 (1974).
[32]U. Berg (private communication).
[33]Cary N. Davids, David R. Goosman, David E. Alburger, A. Gallmann, G. Guillaume, D. H. Wilkinson, and W. A. Langford, Phys. Rev. C 9, 216 (1974).
[34]N. Anantaraman, H. E. Gove, J. P. Trentelman, J. P. Draayer, and F. C. Jundt, Nucl. Phys. A 276, 119 (1977).
[35]K. P. Lieb, Nucl. Phys. 85, 461 (1966).
[36]K. W. Jones, A. Z. Schwarzschild, E. K. Warburton, and D. B. Fossan, Phys. Rev. 178, 1773 (1969).
[37]R. J. Nickles, Nucl. Phys. A 134, 308 (1968).
[38]D. Schwalm and B. Povh, in *Proceedings of the International Conference on Properties of Nuclear States* (Les Presses de l'Université de Montreal, Montreal, Canada, 1969), p. 786.
[39]Franklin D. Snyder, Phys. Rev. C 6, 204 (1972).
[40]H. Sztark, J. L. Quebert, P. Gil, and L. Marquez, J. Phys. (Paris) 33, 841 (1972).
[41]D. S. Andreyev, A. P. Grinberg, K. I. Erokhina, and Ikh. Lemberg, Nucl. Phys. 19, 400 (1960).
[42]N. Nakai, K. S. Stephens, and R. M. Diamond, Nucl. Phys. A 150, 114 (1970).
[43]D. K. Olsen, W. R. Phillips, and A. R. Barnett, Phys. Lett. 39B, 201 (1972).